Commun Nonlinear Sci Numer Simulat 14 (2009) 2144–2159

Contents lists available at ScienceDirect

Commun Nonlinear Sci Numer Simulat

journal homepage: www.elsevier.com/locate/cnsns

A general approach to get series solution of non-similarity boundary-layer flows

Shi-Jun Liao

Sate Key Lab of Ocean Engineering, School of Naval Architecture, Ocean and Civil Engineering, Shanghai Jiao Tong University, Shanghai 200030, China

ARTICLE INFO

Article history:
Received 17 June 2008
Accepted 17 June 2008
Available online 26 June 2008

PACS:
47.15.Cb
02.30.Lt
02.60.Lj

Keywords:
Non-similarity
Boundary-layer
Series solution
Homotopy analysis method
Non-linear PDE with variable coefficient

ABSTRACT

An analytic method for strongly non-linear problems, namely the homotopy analysis method (HAM), is applied to give convergent series solution of non-similarity boundary-layer flows. As an example, the non-similarity boundary-layer flows over a stretching flat sheet are used to show the validity of this general analytic approach. Without any assumptions of small/large quantities, the corresponding non-linear partial differential equation with variable coefficients is transferred into an infinite number of linear ordinary differential equations with constant coefficients. More importantly, an auxiliary artificial parameter is used to ensure the convergence of the series solution. Different from previous analytic results, our series solutions are convergent and valid for all physical variables in the whole domain of flows. This work illustrates that, by means of the homotopy analysis method, the non-similarity boundary-layer flows can be solved in a similar way like similarity boundary-layer flows. Mathematically, this analytic approach is rather general in principle and can be applied to solve different types of non-linear partial differential equations with variable coefficients in science and engineering.

1. Introduction

Since Prandtl [1] proposed the revolutionary concept of boundary-layer flows of viscous fluid in 1904, the boundary-layer theory [2–11] has been developing greatly and applied in nearly all regions of fluid mechanics. When similarity solutions exist, the boundary-layer flows are governed by ordinary differential equations (ODEs), which are much easier to solve than the original partial differential equations (PDEs). Owing to this mathematical simplicity, most researchers focused on similarity boundary-layer flows: in contrast to the large number of publications in similarity boundary-layer flows [9–11], articles on non-similarity flows are much less.

Without loss of generality, let us consider here the non-similarity boundary-layer flows of Newtonian fluids over a stretching flat sheet [12–22], which have important engineering applications such as polymer processing unit in a chemical plant, metal working process in metallurgy and aerodynamic extrusion of plastic sheets. This kind of flow is used here as an example to show the validity of the analytic approach which has general meanings. Two forces in opposite directions with same magnitude are added along the sheet. Thus, there is a rest point on the sheet, which is defined as the origin of the coordinate system. The x and y axis are along and perpendicular to the sheet, respectively. The fluid is at rest far from the sheet (i.e., as $y \to +\infty$). Due to the symmetry of flows, we can only consider the flows in the upper quarter plane $x \geqslant 0,\ y \geqslant 0$. Let $U_w(x)$ denote the stretching velocity of the sheet, (u, v) the velocity components of the fluid, v the kinematic viscosity of the fluid, respectively. As mentioned by Prandtl [1], the velocity variation across the flow direction is much larger than that in

E-mail address: sjliao@sjtu.edu.cn

1007-5704/$ - see front matter © 2008 Elsevier B.V. All rights reserved.
doi:10.1016/j.cnsns.2008.06.013

the flow direction, so that there exists a thin boundary-layer near the sheet. In the frame of the boundary-layer theory, the flows are governed by

$$\frac{\partial u}{\partial x}+\frac{\partial v}{\partial y}=0, \tag{1}$$

$$u\frac{\partial u}{\partial x}+v\frac{\partial u}{\partial y}=\nu\frac{\partial^2 u}{\partial y^2}, \tag{2}$$

subject to the boundary conditions

$$u=U_w(x), \quad v=0 \quad \text{at } y=0, \tag{3}$$

and

$$u=0, \quad \frac{\partial v}{\partial x}=0 \quad \text{at } x=0, \tag{4}$$

$$u\to 0 \quad \text{as } y\to+\infty. \tag{5}$$

The similarity solutions exist only in some special cases of $U_w(x)$. Following Görtler [23], we define the so-called principal function

$$\Lambda(x)=\frac{U_w'(x)}{U_w^2(x)}\int_0^x U_w(\xi)\mathrm{d}\xi. \tag{6}$$

It is easy to find out that, when $\Lambda(x)$ equals to a constant β, i.e.,

$$\frac{U_w'(x)}{U_w^2(x)}\int_0^x U_w(\xi)\mathrm{d}\xi=\beta, \tag{7}$$

there exists the similarity solution

$$\psi=\sqrt{\nu\int_0^x U_w(\xi)\mathrm{d}\xi}\,g(\eta), \quad \eta=\frac{U_w(x)}{\sqrt{\nu\int_0^x U_w(\xi)\mathrm{d}\xi}}y, \tag{8}$$

in which ψ is stream function, and $g(\eta)$ is governed by an ODE

$$g'''+\frac{1}{2}gg''-\beta g'^2=0, \tag{9}$$

subject to the boundary conditions

$$g(0)=0, \quad g'(0)=1, \quad g'(+\infty)=0. \tag{10}$$

The corresponding local coefficient of skin friction is given by

$$C_f=\frac{\tau_w}{\frac{1}{2}\rho U_w^2(x)}=2g''(0)\sqrt{\frac{\nu}{\int_0^x U_w(\xi)\mathrm{d}\xi}}. \tag{11}$$

For example, in case of $U_w(x)=ax^\lambda$, where $a(1+\lambda)>0$, it holds $\beta=\lambda/(1+\lambda)$, and then the similarity criteria (7) is satisfied and thus there exists the similarity solution

$$\psi=\sqrt{\frac{a\nu}{(1+\lambda)}}x^{\frac{\lambda+1}{2}}g(\eta), \quad \eta=\sqrt{\frac{a(1+\lambda)}{\nu}}x^{\frac{\lambda-1}{2}}y. \tag{12}$$

In this way, the system of the two coupled non-linear PDEs becomes an ODE, which is much easier to solve than the original PDEs. So, when similarity solutions exist, the problem is greatly simplified from the viewpoint of mathematics.

For similarity boundary-layer flows, velocity profiles at different x are *similar*. However, such kind of similarity is lost for non-similarity flows [24–29]. Physically speaking, the non-similarity boundary-layer flows are more general in nature and in our everyday life, and thus are more important than similarity ones. As mentioned by Sparrow et al. [26], the non-similarity may be caused by (a) spatial variations in the free stream velocity, (b) sheet mass transfer, and (c) transverse curvature. How about the evolution of velocity profiles, local coefficient of skin friction and boundary-layer thickness of non-similarity flows? Are there any relationships between the similarity and non-similarity boundary-layer flows? To answer these questions, we had to directly investigate non-similarity boundary-layer flows.

When similarity solutions do not exist, one had to solve a non-linear PDE. From mathematical viewpoints, it is much more difficult to solve a non-linear PDE than ODE. There are two different approaches: analytic and numerical ones. In the investigation of non-similarity boundary-layer flows, numerical methods are widely applied. As shown in [30–37], one can use numerical methods to obtain approximate results at a large number of discretized points. However, one had to replace the infinite domain by a finite ones, and this brings some additional errors and uncertainty into the numerical results. By

means of analytical methods, one can solve the non-linear PDEs in the infinite domain. However, it is a pity that, using the traditional analytic techniques such as perturbation techniques, it is hard to get analytic approximations that are valid and accurate for *all* physical variables. This is mainly because perturbation methods are often dependent on small variables or parameters, and thus perturbation results are generally not valid for *all* possible physical parameters/variables. Currently, Cimpean et al. [29] applied the perturbation techniques, combined with numerical techniques, to solve a free convection non-similarity boundary-layer problem over a vertical flat sheet in a porous medium. Like most of perturbation solutions, their results are valid only for small and large x, which are regarded as perturbation quantities. Among the analytic methods for non-similarity thermal boundary-layer problems, "the method of local similarity" [27,28] seems to be most frequently applied, owing to its conceptual and computational simplicity. By means of "the method of local similarity", one assumes that the non-similarity terms in governing equations are small enough so that they can be regarded as zero, and then the original PDEs become an ODE. However, the results given by "the method of local similarity" are of "uncertain accuracy", as pointed out by Sparrow et al. [27], and is valid only for small ξ in general, as pointed out by Massoudi [28]. These conclusions are easy to understand, because non-similarity terms are certainly *not* zero and must be considered. Sparrow et al. [24,26,27] introduced the so-called "method of local non-similarity", which was currently applied by Massoudi [28] to solve a non-similarity flows of non-Newtonian fluid over a wedge. Differentiating the original governing equations by the dimensionless variable ξ along the free stream velocity, Massoudi [28] gave two additional auxiliary non-linear PDEs for both momentum and energy equations, then regarded the variable ξ in these two PDEs to be a *constant* so as to reduce them as a system of ODEs, and finally used numerical techniques to solve the more complicated system of four equations, i.e., the two original PDEs plus the two auxiliary PDEs. In some cases, the results given by "the method of local non-similarity" agree well with numerical or series solutions, as reported in [24,25]. However, it is a pity that Massoudi [28] only gave numerical results for small ξ ($\xi \leqslant 0.4$). Owing to above-mentioned mathematical difficulties, the publications in non-similarity boundary-layer flows are much less than those in similarity ones, although the former seems more important not only in theory but also in applications.

Based on homotopy, which is a basic concept in topology, a analytic method, namely the homotopy analysis method (HAM) [38–42], is proposed and then widely applied to solve strongly non-linear problems in science, engineering and finance [43–56]. Unlike perturbation techniques, the homotopy analysis method is independent of any small/large physical parameters. Besides, different from perturbation and traditional non-perturbation methods, it provides a simple way to ensure the convergence of solution series so that one can always get accurate enough approximations even for strongly non-linear problems. Furthermore, unlike all other analytic techniques, the homotopy analysis method provides great freedom to choose the so-called auxiliary linear operator so that one can approximate a non-linear problem more effectively by means of better base functions. This kind of freedom is so large that the second-order non-linear two-dimensional Gelfand equation can be solved even by means of a fourth-order auxiliary linear operator, as shown in [41]. Especially, by means of the homotopy analysis method, a few new solutions of some non-linear problems [54,55] are found, which are neglected by all other analytic methods and even by numerical techniques. Furthermore, the homotopy analysis method has been applied to solve some non-linear partial differential equations, such as unsteady similarity boundary-layer flows [40], Black–Scholes type equation in finance for American put option [52,53] and interaction of non-linear water wave and exponential shear currents [56]. These previous work provide us a good background to apply the HAM to solve non-linear PDEs with variable coefficients.

In this paper, we provide a general analytic approach to solve non-similarity boundary-layer flows through a typical example. In Section 2, the basic ideas of the analytic approach are described. In Section 3, two kinds of non-similarity flows are investigated and the accurate series solutions are obtained, which are convergent and valid in the whole spatial regions. In Section 4, an approximate formula of local coefficient of skin friction is provided for general non-similarity flows, which gives rather accurate results for all physical parameters. Discussions and conclusions are given in Section 5.

2. Analytic approach based on the HAM

When $U_w(x)$ does not satisfy the similarity criteria (7), we had to solve a non-linear PDE. Using the streamfunction ψ, the non-similarity boundary-layer flows are governed by

$$\nu \frac{\partial^3 \psi}{\partial y^3} + \frac{\partial \psi}{\partial x}\frac{\partial^2 \psi}{\partial y^2} - \frac{\partial \psi}{\partial y}\frac{\partial^2 \psi}{\partial x \partial y} = 0, \tag{13}$$

subject to the boundary conditions

$$\psi = 0, \quad \frac{\partial \psi}{\partial y} = U_w(x) \quad \text{at } y = 0, \quad \frac{\partial \psi}{\partial y} \to 0 \quad \text{as } y \to +\infty. \tag{14}$$

Using the transformation

$$\eta = \frac{y}{\nu^{1/2}\sigma(x)}, \quad \psi = \nu^{1/2}\sigma(x) f(x,\eta), \tag{15}$$

where $\sigma(x) > 0$ is a real function to be chosen later, one has

$$u=\frac{\partial f}{\partial \eta},\quad v=v^{1/2}\left[\sigma'(x)\left(\eta\frac{\partial f}{\partial \eta}-f\right)-\sigma(x)\frac{\partial f}{\partial x}\right].$$

Then, the governing equation becomes

$$\frac{\partial^3 f}{\partial \eta^3}+\frac{1}{2}[\sigma^2(x)]'f\frac{\partial^2 f}{\partial \eta^2}+\sigma^2(x)\left(\frac{\partial f}{\partial x}\frac{\partial^2 f}{\partial \eta^2}-\frac{\partial f}{\partial \eta}\frac{\partial^2 f}{\partial x\partial \eta}\right)=0, \tag{16}$$

subject to the boundary conditions

$$f(x,0)=0,\quad f_\eta(x,0)=U_w(x),\quad f_\eta(x,+\infty)=0, \tag{17}$$

where f_η denotes the partial derivative with respect to η. Note that Eq. (16) is a non-linear PDE with *variable* coefficient $\sigma^2(x)$, and besides Eq. (15) is *not* the traditional similarity transformation.

There are an infinite number of sheet stretching velocity $U_w(x)$ which does not satisfy the similarity-criteria (7). Here, without loss of generality, let us consider the case $U_w(x)=U_w(\xi)$, where $\xi=\Gamma(x)$ is a given real function of x. By means of the transformation[1]

$$\xi=\Gamma(x), \tag{18}$$

Eq. (16) becomes

$$\frac{\partial^3 f}{\partial \eta^3}+\sigma_1(\xi)f\frac{\partial^2 f}{\partial \eta^2}+\sigma_2(\xi)\left(\frac{\partial f}{\partial \xi}\frac{\partial^2 f}{\partial \eta^2}-\frac{\partial f}{\partial \eta}\frac{\partial^2 f}{\partial \xi\partial \eta}\right)=0, \tag{19}$$

subject to the boundary conditions

$$f(\xi,0)=0,\quad f_\eta(\xi,0)=U_w(\xi),\quad f_\eta(\xi,+\infty)=0, \tag{20}$$

where

$$\sigma_1(\xi)=\frac{1}{2}[\sigma^2(x)]',\quad \sigma_2(\xi)=\Gamma'(x)\sigma^2(x),$$

in which x is expressed by ξ, i.e., $x=\Gamma^{-1}(\xi)$.

The corresponding local coefficient of skin friction of non-similarity flows is given by

$$C_f(x)=\frac{\tau(x)}{\frac{1}{2}\rho U_w^2(x)}=\frac{2v^{1/2}}{\sigma(x)U_w^2(x)}\frac{\partial^2 f}{\partial \eta^2}\bigg|_{\eta\to 0}. \tag{21}$$

So, it is important to get accurate results of $f_{\eta\eta}(\xi,0)$. The replacement boundary-layer thickness $\delta(x)$ is defined by

$$\delta(x)U_w(x)=\int_0^{+\infty}u(x,y)\mathrm{d}y,$$

which gives

$$\delta(x)=\frac{1}{U_w(x)}\int_0^{+\infty}u(x,y)\mathrm{d}y. \tag{22}$$

For the sake of simplicity, define a non-linear operator

$$\mathscr{N}f=\frac{\partial^3 f}{\partial \eta^3}+\sigma_1(\xi)f\frac{\partial^2 f}{\partial \eta^2}+\sigma_2(\xi)\left(\frac{\partial f}{\partial \xi}\frac{\partial^2 f}{\partial \eta^2}-\frac{\partial f}{\partial \eta}\frac{\partial^2 f}{\partial \xi\partial \eta}\right). \tag{23}$$

Let $q\in[0,1]$ denote an embedding parameter, $\hbar\neq 0$ an auxiliary parameter (called convergence-control parameter [42]), $\mathscr{L}$ an auxiliary linear operator and $f_0(\xi,\eta)$ an initial guess that satisfies the boundary conditions (20), respectively. Here, the auxiliary linear operator $\mathscr{L}$ has the properties

$$\mathscr{L}[0]=0 \tag{24}$$

and

$$\mathscr{L}[\alpha_1(q)w_1(\xi,\eta;q)+\alpha_2(q)w_2(\xi,\eta;q)]=\alpha_1(q)\mathscr{L}[w_1(\xi,\eta;q)]+\alpha_2(q)\mathscr{L}[w_2(\xi,\eta;q)], \tag{25}$$

where $\alpha_1(q),\ \alpha_2(q),\ w_1(\xi,\eta;q)$ and $w_2(\xi,\eta;q)$ are any real functions. Both $\mathscr{L}$ and $f_0(\xi,\eta)$ will be chosen later. Here, we just emphasize that we have great freedom to choose the auxiliary linear operator $\mathscr{L}$ and the initial guess $f_0(\xi,\eta)$. Then, we construct the so-called zeroth-order deformation equation

[1] Note that, if $\Gamma(x)=x$, then $\xi=x$ and $U_w(\xi)=U_w(x)$. So, our approach described below is valid for any $U_w(x)$ in general.

$$(1-q)\mathscr{L}[F(\xi,\eta,q)-f_0(\xi,\eta)]=q\hbar\mathscr{N}[F(\xi,\eta,q)], \tag{26}$$

subject to the boundary conditions on the sheet

$$F(\xi,0,q)=0,\quad F_\eta(\xi,0,q)=U_w(\xi), \tag{27}$$

and the boundary condition at infinity

$$F_\eta(\xi,+\infty,q)\to 0. \tag{28}$$

Note that $f_0(\xi,\eta)$ satisfies the boundary conditions (20) and $\mathscr{L}$ has the property (24). Thus, when $q=0$, the solution of Eqs. (26)–(28) reads

$$F(\xi,\eta,0)=f_0(\xi,\eta). \tag{29}$$

When $q=1$, since $\hbar\neq 0$, Eqs. (26)–(28) are equivalent to Eqs. (19) and (20), provided

$$F(\xi,\eta,1)=f(\xi,\eta). \tag{30}$$

Thus, as the embedding parameter q increases from 0 to 1, $F(\xi,\eta,q)$ varies *continuously* from the initial guess $f_0(\xi,\eta)$ to the exact solution $f(\xi,\eta)$ of Eqs. (19) and (20). This kind of continuous variation (or deformation) is called homotopy in topology. That is the reason why we call Eqs. (26)–(28) the zeroth-order deformation equation. Expanding $F(\xi,\eta,q)$ in Taylor series with respect to q and using (29), we have

$$F(\xi,\eta,q)=f_0(\xi,\eta)+\sum_{m=1}^{+\infty}f_m(\xi,\eta)q^m, \tag{31}$$

where

$$f_m(\xi,\eta)=\frac{1}{m!}\frac{\partial^m F(\xi,\eta,q)}{\partial q^m}\bigg|_{q=0}.$$

Note that, the convergence of the series (31) depends on the initial guess $f_0(\xi,\eta)$, the auxiliary linear operator $\mathscr{L}$ and the auxiliary parameter $\hbar$. Assuming that all of them are properly chosen so that the series (31) converges at $q=1$, we have due to (30) the series solution

$$f(\xi,\eta)=f_0(\xi,\eta)+\sum_{m=1}^{+\infty}f_m(\xi,\eta). \tag{32}$$

This provides us a relationship between the initial guess $f_0(\xi,\eta)$ and the exact solution $f(\xi,\eta)$.

The governing equation and boundary conditions of $f_m(\xi,\eta)$ are deduced directly from the zeroth-order deformation equations (26)–(28). For simplicity, write

$$\vec{f}_k=\{f_0(\xi,\eta),f_1(\xi,\eta),f_2(\xi,\eta),\ldots,f_k(\xi,\eta)\}.$$

Based on the definition of $f_m(\xi,\eta)$, Liao [38] provided a general approach to give governing equations and boundary conditions for $f_m(\xi,\eta)$. Currently, Sajid et al. [51] suggested an equivalent approach: directly substituting the series (31) into the zeroth-order deformation equations (26)–(28), and equating the coefficient of the like-power of q, one obtains the mth-order deformation equation

$$\mathscr{L}\left[f_m(\xi,\eta)-\chi_m f_{m-1}(\xi,\eta)\right]=\hbar R_m(\vec{f}_{m-1}), \tag{33}$$

subject to the boundary conditions on the sheet

$$f_m=0,\quad \frac{\partial f_m}{\partial\eta}=0,\quad \text{at } y=0 \tag{34}$$

and the boundary condition at infinity

$$\frac{\partial f_m}{\partial\eta}\to 0\quad \text{as } y\to+\infty, \tag{35}$$

where

$$R_m(\vec{f}_{m-1})=\frac{\partial^3 f_{m-1}}{\partial\eta^3}+\sigma_1(\xi)\sum_{n=0}^{m-1}f_{m-1-n}\frac{\partial^2 f_n}{\partial\eta^2}+\sigma_2(\xi)\sum_{n=0}^{m-1}\left(\frac{\partial f_n}{\partial\xi}\frac{\partial^2 f_{m-1-n}}{\partial\eta^2}-\frac{\partial f_n}{\partial\eta}\frac{\partial^2 f_{m-1-n}}{\partial\xi\partial\eta}\right) \tag{36}$$

and

$$\chi_m=\begin{cases}0, & m\leqslant 1,\\ 1, & m>1.\end{cases} \tag{37}$$

The above equations are exactly the same as those given by Liao's approach [38]. For details, please refer to Liao [41,42] and Sajid et al. [51]. It should be emphasized here that the high-order deformation equations (33)–(35) are *linear*. Besides, unlike perturbation techniques, we do *not* need any small/large parameters to obtain these linear differential equations. Furthermore, different from "the method of local similarity" and "the method of local non-similarity", we neither enforce the non-similarity terms to be zero, nor regard the variable ξ as a constant. Finally, as mentioned before, we have great freedom to choose $\mathscr{L}$. This freedom is so large that, in the frame of the HAM, a system of non-linear PDEs can be sometimes transferred into an infinite number of linear ODEs. We will illustrate this point soon.

Now, let us choose the initial guess $f_0(\xi,\eta)$ and the auxiliary linear operator $\mathscr{L}$. Mathematically, the essence to approximate a non-linear differential equation is to find a set of *proper* base functions to fit its solutions. Physically, it is well-known that most viscous flows decay exponentially at infinity (i.e., $y \to +\infty$). So, for non-similarity boundary-layer flows over a stretching flat sheet, the velocities u and v should decay exponentially at infinity (i.e., $y \to +\infty$). So, even if we do not know now the details of the solution $f(\xi,\eta)$, we are quite sure that the solution $f(\xi,\eta)$ should be in such a form

$$f(\xi,\eta) = \sum_{m=0}^{+\infty} \sum_{n=0}^{+\infty} a_{m,n} \xi^n \exp(-m\eta), \tag{38}$$

where $a_{m,n}$ is constant coefficient to be determined. It is well-known that the velocity of Blasius' similarity boundary-layer flows [2] decays like $\exp(-\eta^2)$ far from the sheet, which is faster than $\exp(-my)$ for any real number $m > 0$. However, it has been found that the steady/unsteady similarity boundary-layer flows of Newtonian/non-Newtonian fluid over a stretching flat sheet can be expressed in forms similar to (38) and the corresponding series solutions agree well with numerical ones, as shown in [39,54,55]. So, we are quite sure that the non-similarity boundary-layer flows can be expressed by (38). Our purpose is to give convergent series solution of the non-linear PDEs (19) and (20), expressed in the form (38). Note that, the above expression, namely *the solution expression* of $f(\xi,\eta)$, is rather important in the frame of the HAM, as shown below.

To satisfy the solution expression (38) and the boundary conditions (20), we choose the initial guess

$$f_0(\xi,\eta) = U_w(\xi)(1 - \mathrm{e}^{-\eta}), \tag{39}$$

which contains the simplest but leading terms (as $\eta \to +\infty$) in (38). Note that $f_0(\xi,\eta)$ satisfies the boundary conditions (20) and decays exponentially as $\eta \to +\infty$. Due to the freedom on the choice of the initial guess, one can add more additional terms in $f_0(\xi,\eta)$, but the above initial guess is good enough for our current purpose, as shown later.

As mentioned before, we have great freedom to choose the auxiliary linear operator $\mathscr{L}$. However, this freedom is restricted by the solution expression (38) and the boundary conditions (20), which we must consider in the choice of $\mathscr{L}$. Note that the original governing equation (19) is a non-linear PDE with variable coefficients. So, if we choose $\mathscr{L}$ as a partial differential operator, the high-order deformation equation (33) is a partial differential ones. It is well-known that, in general, a PDE with variable coefficients is more difficult to solve than an ODE with constant coefficients. So, mathematically, it is much easier to solve Eq. (33) if we could choose $\mathscr{L}$ as an linear differential operator which contains derivatives only with respect to ξ or η, but does not contain any variable coefficients. Physically, for boundary-layer flows, the velocity variation across the flow direction is much larger than that in the flow direction. Therefore, the derivatives $\frac{\partial f_m}{\partial \eta}$, $\frac{\partial^2 f_m}{\partial \eta^2}$, $\frac{\partial^3 f_m}{\partial \eta^3}$ are considerably larger and thus physically more important than $\frac{\partial f_m}{\partial \xi}$, $\frac{\partial^2 f_m}{\partial \xi \partial \eta}$. Considering all of these mentioned above, we choose the auxiliary linear operator

$$\mathscr{L} w = \frac{\partial^3 w}{\partial \eta^3} + a_2(\xi)\frac{\partial^2 w}{\partial \eta^2} + a_1(\xi)\frac{\partial w}{\partial \eta} + a_0(\xi) w, \tag{40}$$

where $a_0(\xi)$, $a_1(\xi)$ and $a_2(\xi)$ are real functions to be determined. Let $w_1^*(\eta,\xi)$, $w_2^*(\eta,\xi)$ and $w_3^*(\eta,\xi)$ denote the three non-zero solutions of $\mathscr{L} w = 0$, i.e.,

$$\mathscr{L}[w_1^*(\eta,\xi)] = \mathscr{L}[w_2^*(\eta,\xi)] = \mathscr{L}[w_3^*(\eta,\xi)] = 0. \tag{41}$$

Then, the general solution of the high-order deformation equations (33) is given by

$$f_m(\eta,\xi) = f_m^*(\eta,\xi) + C_1(\xi) w_1^*(\eta,\xi) + C_2(\xi) w_2^*(\eta,\xi) + C_3(\xi) w_3^*(\eta,\xi), \tag{42}$$

where $f_m^*(\eta,\xi)$ is a special solution of (33), and $C_1(\xi)$, $C_2(\xi)$, $C_3(\xi)$ are real functions determined by the boundary conditions (34) and (35). The special solutions $w_1^*(\eta,\xi)$, $w_2^*(\eta,\xi)$ and $w_3^*(\eta,\xi)$ should be chosen in such a way that the above solution $f_m(\eta,\xi)$ obeys the so-called solution expression (38), and besides the boundary conditions (34) and (35) are satisfied. Obviously, if the special solutions $w_1^*(\eta,\xi)$, $w_2^*(\eta,\xi)$ and $w_3^*(\eta,\xi)$ are *independent* of ξ, then Eq. (33) becomes an ODE with *constant* coefficients and thus is easy to solve. There are many ways to do so. For example, according to the solution expression (38), we can choose

$$w_1^* = 1, \quad w_2^* = \exp(-\eta), \quad w_3^* = \exp(-2\eta).$$

In this case, the general solution of Eq. (33) reads

$$f_m(\eta,\xi) = f_m^*(\eta,\xi) + C_1 + C_2 \exp(-\eta) + C_3 \exp(-2\eta). \tag{43}$$

The above expression automatically satisfies the boundary condition (35) at infinity, thus only two integral coefficients can be determined so that the solution of Eq. (33) is *not* unique. To avoid this, we replace $w_3^* = \exp(-2\eta)$ by $w_3^* = \exp(\eta)$. Then, the general solution of Eq. (33) becomes

$$f_m(\eta,\xi) = f_m^*(\eta,\xi) + C_1 + C_2\exp(-\eta) + C_3\exp(\eta). \tag{44}$$

To satisfy the boundary condition (35) at infinity, it holds $C_3 = 0$. Then, the integral coefficients C_1 and C_2 are uniquely determined by the two boundary conditions (34) on the sheet. In this way, the solution of the high-order deformation equations (33)–(35) is *unique*, and satisfies all of the boundary conditions (34) and (35), but does *not* disobey the so-called solution expression (38). Finally, using the definition (40) of $\mathscr{L}$, and substituting

$$w_1^*(\xi,\eta) = 1, \quad w_2^*(\xi,\eta) = \exp(-\eta), \quad w_3^*(\xi,\eta) = \exp(\eta)$$

into (41), we have a set of algebraic equations

$$\begin{aligned} &a_0(\xi) = 0,\\ &-1 + a_2(\xi) - a_1(\xi) + a_0(\xi) = 0,\\ &1 + a_2(\xi) + a_1(\xi) + a_0(\xi) = 0, \end{aligned}$$

whose solution reads

$$a_0(\xi) = 0, \quad a_1(\xi) = -1, \quad a_2(\xi) = 0.$$

Substituting them into (40), we have the auxiliary linear operator

$$\mathscr{L}f = \frac{\partial^3 f}{\partial\eta^3} - \frac{\partial f}{\partial\eta}, \tag{45}$$

which does not contain any variable coefficients. Due to the freedom on the choice of $\mathscr{L}$, it is possible for us to use $w_3^* = \exp(\kappa\eta)$, where $\kappa \geqslant 1$ is a positive integer, to define $\mathscr{L}$ in other forms. Besides, the order of $\mathscr{L}$ might be even not equal to 3, as pointed out by Liao and Tan [41]. So, there might exist the best auxiliary linear operator $\mathscr{L}$ among all of these possible ones. However, for the purpose of this paper, although the auxiliary linear operator (45) might be not the best, it is good enough for our purpose, as described later.

Now, under the definition (39) of the initial guess and the definition (45) of the auxiliary linear operator $\mathscr{L}$, it is easy to solve the *linear* ODEs (33) to (35) which contains only *constant* coefficients. The special solution of (33) reads

$$f_m^*(\xi,\eta) = \chi_m f_{m-1}(\xi,\eta) + \hbar\mathscr{L}^{-1}[R_m(\vec{\psi}_{m-1})], \tag{46}$$

where $\mathscr{L}^{-1}$ denotes the inverse operator of $\mathscr{L}$. According to the definition (45), we have

$$\mathscr{L}^{-1}[\gamma(\xi)\exp(-m\eta)] = \frac{\gamma(\xi)\exp(-m\eta)}{m(1-m^2)} \tag{47}$$

for any a real function $\gamma(\xi)$ and positive integer $m \geqslant 1$. Besides, $\mathscr{L}^{-1}$ has the linear property

$$\mathscr{L}^{-1}[\beta_1(\xi)g_1(\eta) + \beta_2(\xi)g_2(\eta)] = \beta_1(\xi)\mathscr{L}^{-1}[g_1(\eta)] + \beta_2(\xi)\mathscr{L}^{-1}[g_2(\eta)] \tag{48}$$

for any real functions $\beta_1(\xi)$, $\beta_2(\xi)$, $g_1(\eta)$ and $g_2(\eta)$. Then, the solution of the high-order deformation Eqs. (33)–(35) is

$$f_m(\xi,\eta) = f_m^*(\eta,\xi) + C_0 + C_1\exp(-\eta),$$

where

$$C_0 = -f_m^*(\xi,0) - \left.\frac{\partial f_m^*}{\partial\eta}\right|_{\eta=0}, \quad C_1 = \left.\frac{\partial f_m^*}{\partial\eta}\right|_{\eta=0}$$

are determined by the boundary conditions (34) and (35). Thus, using (46)–(48), it is rather easy to solve the high-order deformation equations (33)–(35), especially by means of symbolic software such as Mathematica, MathLab and Maple.

Finally, it should be emphasized that $f_m(\xi,\eta)$ contains the auxiliary parameter $\hbar$, called the convergence-control parameter. As pointed out in the previous work [38–40,44–49,51], it is the auxiliary parameter $\hbar$ which provides us with a simple way to ensure the convergence of the series solution for *all* physical variables/parameters. We will show this point in Section 3.

3. Series solution of two non-similarity flows

There are an infinite number of sheet velocities $U_w(x)$ that do not satisfy the similarity criteria (7) and thus lead to non-similarity boundary-layer flows. Without loss of generality, let us consider here two sheet stretching velocities listed

Table 1
Surface stretching velocity and the related criterion function $\Delta(x)$

	$U_w(x)$	$\Delta(x)$
Example 1	$\frac{x}{1+x}$	$\frac{x-\ln(1+x)}{x^2}$
Example 2	$\frac{x}{(1+x)} - \frac{x^2}{2(1+x)^2}$	$\frac{2}{(x+2)^2}$

in Table 1. Recall that $\Delta(x) =$ constant is the criterion of existence of similarity solutions. So, according to Table 1, there are no similarity solutions. Note that the two sheet stretching velocities considered here tend to a constant as $x \to +\infty$. This is reasonable, because $U_w(x)$ is often bounded in practice.

3.1. Example 1: $U_w = x/(1+x)$

In this case, the stretching velocity $U_w(x)$ increases monotonously from 0 to 1 along the sheet. Note that $U_w \to x$ as $x \to 0$, and $U_w \to 1$ as $x \to +\infty$, respectively. Physically, the flows near $x = 0$ should be close to the similarity ones with $U_w = x$, and besides, the flows as $x \to +\infty$ should be close to the similarity ones with $U_w = 1$, respectively. For similarity flows with $U_w = x$ and $U_w = 1$, the similarity variables are $y/\sqrt{v}$ and $y/\sqrt{vx}$, respectively. Therefore, according to the definition (15) of the variable η, we choose

$$\sigma(x) = \sqrt{1+x},$$

so that η tends to $y/\sqrt{v}$ as $x \to 0$, and to $y/\sqrt{vx}$ as $x \to +\infty$, respectively.

For the sake of simplicity, we define

$$\xi = \Gamma(x) = \frac{x}{1+x},$$

which gives

$$U_w = \xi, \quad \sigma_1(\xi) = \frac{1}{2}, \quad \sigma_2(\xi) = 1 - \xi.$$

Using symbolic computation software (such as Mathematica), it is easy to solve the system of the linear ODEs (33)–(35) (with constant coefficients) to get high-order approximations. Obviously, it is important to ensure the convergence of the solution series (32) for *all* possible physical variables $0 \leqslant x < +\infty$ and $0 \leqslant y < +\infty$. Otherwise, the series solution (32) is useless. Fortunately, our series solution (32) contains the convergence-control parameter $\hbar$, which provides us a simple way to adjust and control the convergence region and rate of series solution, as mentioned by Liao [38–40] and others [44–49,51]. To show this, let us first consider $f_{\eta\eta}(\xi, 0)$, which is closely related to the local coefficient of skin friction via (21). Note that, *mathematically*, $f_{\eta\eta}(\xi, 0)$ is a function of the physical variable ξ and the convergence-control parameter $\hbar$. For a given value of ξ, $f_{\eta\eta}(\xi, 0)$ is a power series of $\hbar$ and thus its convergence is determined by $\hbar$. However, *physically*, for a given value of ξ, the local coefficient of skin friction is unique, i.e., there should exist *one and only one* value of $f_{\eta\eta}(\xi, 0)$ (we assume here that no multiple solutions exist). Therefore, for given ξ, *all* convergent series solutions of $f_{\eta\eta}(\xi, 0)$ given by *different* values of $\hbar$ should converge to the *same* value. So, regarding $\hbar$ as a variable, we can plot the curves of $f_{\eta\eta}(\xi, 0) \sim \hbar$ for different values of ξ such as $\xi = 1/4$, 1/2, 3/4 and 1, as shown in Fig. 1. At $\xi = 1$, $f_{\eta\eta}(\xi, 0)$ converges to the same value for all $\hbar$ in the region $-1 \leqslant \hbar < -0.25$. At $\xi = 1/4$, it also converges to the same value (which is different from that at $\xi = 1$) when $-1 \leqslant \hbar < -0.25$. However, at $\xi = 1/2$ and 3/4, $f_{\eta\eta}(\xi, 0)$ converges in the region $-0.75 < \hbar < -0.25$ but diverges when $\hbar = -1$. As shown in Fig. 2, when $\hbar = -1$ and -0.9, $f_{\eta\eta}(\xi, 0)$ converges only for small ξ and $\xi = 1$, corresponding to small x and $x \to +\infty$, but diverges in a region $0.5 \leqslant \xi < 1$. Thus, when $\hbar < -0.9$, the series of $f_{\eta\eta}(\xi, 0)$ is divergent if x is neither small nor very large. Fortunately, as illustrated by Liao [38–40] and others [44–49,51], the homotopy analysis method provides us freedom to choose the value of the convergence-control parameter $\hbar$, and therefore we can get series of $f_{\eta\eta}(\xi, 0)$ convergent in the *whole* region $0 \leqslant \xi \leqslant 1$ (corresponding to $0 \leqslant x < +\infty$), simply by choosing $\hbar = -1/2$, as shown in Fig. 2.

Furthermore, it is found that, when $\hbar = -1/2$, our series solution (32) is convergent even for *all* physical variables $0 \leqslant \xi \leqslant 1$ and $0 \leqslant \eta < +\infty$, corresponding to $0 \leqslant x < +\infty$ and $0 \leqslant y < +\infty$. It should be emphasized that, as proved by Liao [38] in general, the HAM solution series converges to solutions of original non-linear PDEs as long as it is not divergent. This is indeed true: our series solution agree well with numerical ones. Note that, as proved by Liao [38], other non-perturbation techniques such as Adomian's decomposition method [57–60], the δ-expansion method [61,62] and Lyapunov's artificial small parameter method [63], are special cases of the homotopy analysis method in case of $\hbar = -1$. So, if these non-perturbation methods are used here, one can *not* get convergent series solution valid in the *whole* upper quarter plane $0 \leqslant x < +\infty$ and $0 \leqslant y < +\infty$.

It is important to give accurate local coefficient of skin friction of non-similarity flows, which is related to $f_{\eta\eta}(\xi, 0)$ via (21). When $\hbar = -1/2$, our 15th-order HAM approximation reads

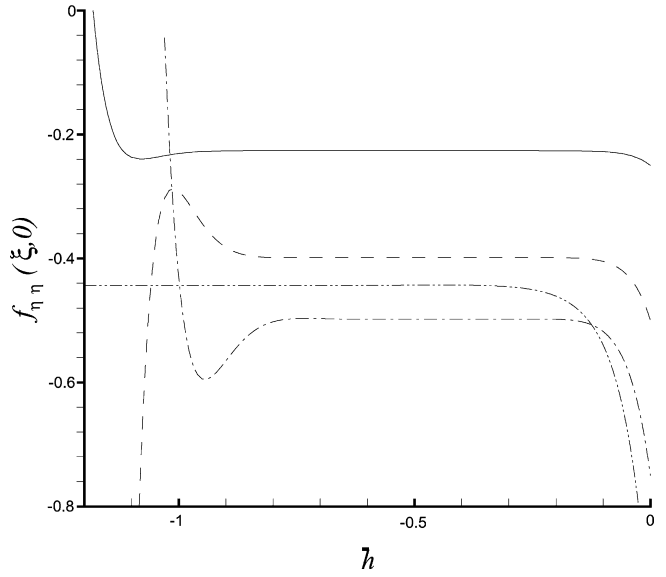

Fig. 1. Curves of the 24th-order approximation of $f_{\eta\eta}(\xi,0)$ versus $\hbar$ in Case A; solid line: $\xi = 1/4$; dashed line: $\xi = 1/2$; dashed-dotted line: $\xi = 3/4$; dash-dot-dotted line: $\xi = 1$.

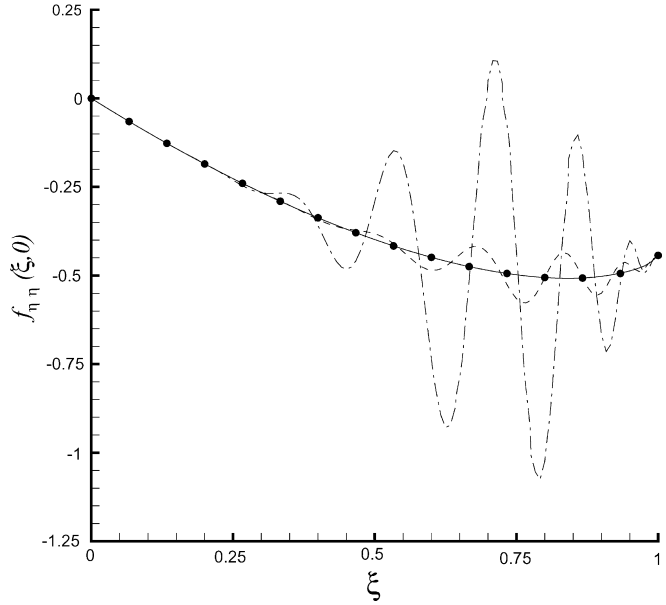

Fig. 2. $f_{\eta\eta}(\xi,0)$ in Case A by means of different values of $\hbar$. Solid line: 18th-order approximation when $\hbar = -1/2$; circles: 24th-order approximation when $\hbar = -1/2$; dashed line: 24th-order approximation when $\hbar = -0.9$; dash-dotted line: 24th-order approximation when $\hbar = -1$.

$$\begin{aligned} f_{\eta\eta}(\xi,0) = &-\xi + 0.357142\xi^2 + 0.0745784\xi^3 + 0.0329563\xi^4 + 0.0187480\xi^5 + 0.0121641\xi^6 + 0.00856336\xi^7 \\ &+ 0.00638095\xi^8 + 0.00468866\xi^9 + 0.0125286\xi^{10} - 0.108975\xi^{11} + 0.729854\xi^{12} - 2.509780\xi^{13} \\ &+ 4.702786\xi^{14} - 4.475992\xi^{15} + 1.690259\xi^{16}, \end{aligned} \tag{49}$$

which agrees well with the 30th-order approximations and is accurate in the whole region $0 \leqslant \xi \leqslant 1$. Knowing the accurate values of $f_{\eta\eta}(\xi,0)$, it is straightforward to calculate the local coefficient of skin friction by (21). It is found that C_f tends to $-2\sqrt{\nu}/x$ as $x \to 0$ and $-0.8875\sqrt{\nu/x}$ as $x \to +\infty$, respectively, as shown in Fig. 3. Besides, the boundary-layer thickness $\delta(x)$ of non-similarity flows tends to $\sqrt{\nu}$ as $x \to 0$ and $1.61613\sqrt{\nu x}$ as $x \to +\infty$, respectively, as shown in Fig. 4. Note that the boundary-layer thickness of similarity flow is $\sqrt{\nu}$ in case of $U_w = x$ and $1.61613\sqrt{\nu x}$ in case of $U_w = 1$, respectively. So, according to our series solution, we have

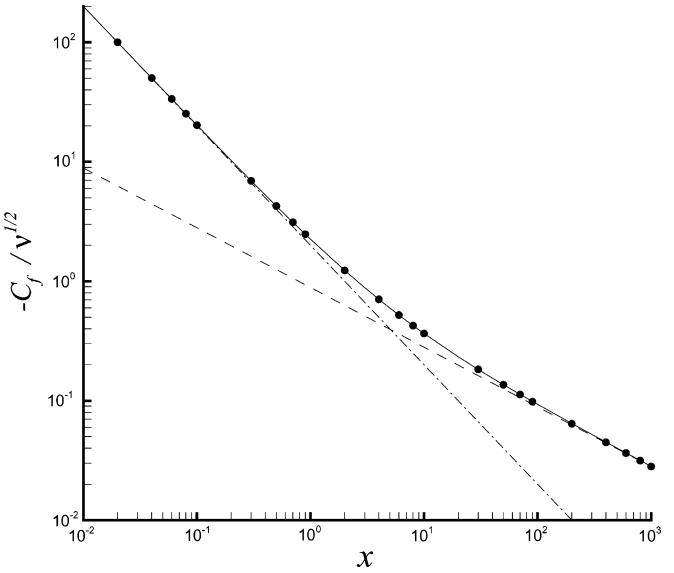

Fig. 3. The local coefficient of skin friction $C_f(x)/\sqrt{v}$ of non-similarity flows in case of $U_w = x/(1+x)$. Solid-line: 30th-order HAM result; symbols: 20th-order HAM result; dashed-line: $C_f(x) = -0.8875\sqrt{v/x}$; dash-dotted line: $C_f(x) = -2\sqrt{v}/x$.

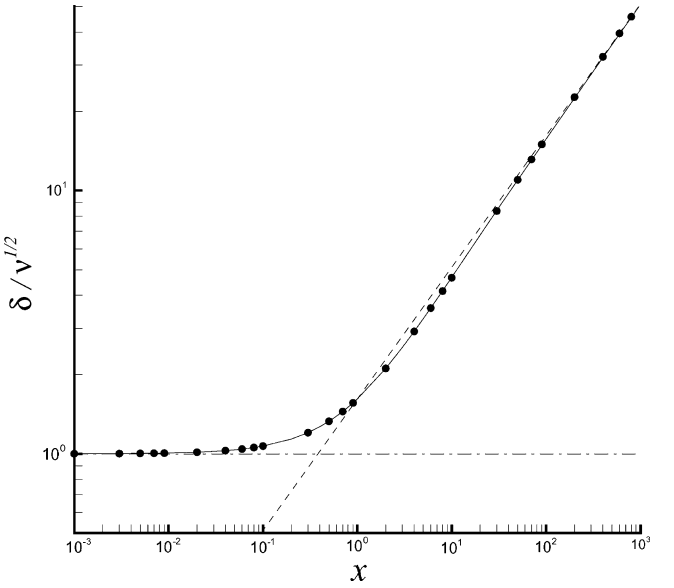

Fig. 4. The boundary-layer thickness $\delta(x)/\sqrt{v}$ of non-similarity flows in case of $U_w = x/(1+x)$. Solid-line: 30th-order HAM result; symbols: 20th-order HAM result; dashed-line: $\delta(x) = 1.61613\sqrt{vx}$; dash-dotted line: $\delta(x) = \sqrt{v}$.

$$C_f(x) \to -2\sqrt{v}/x, \quad \delta(x) \to \sqrt{v} \quad \text{as } x \to 0$$

and

$$C_f(x) \to -0.8875\sqrt{v/x}, \quad \delta(x) \to 1.61613\sqrt{vx} \quad \text{as } x \to +\infty,$$

respectively. Thus, the non-similarity flows in the region $x \to 0$ and $+\infty$ are very close to the similarity ones in case of $U_w = x$ and 1, respectively. However, the flows in other regions are non-similar, as shown in Figs. 3 and 4.

3.2. Example 2: $U_w = x/(1+x) - 0.5x^2/(1+x)^2$

In this case, $U_w \to x$ as $x \to 0$, and $U_w \to 1/2$ as $x \to +\infty$, respectively. Physically, the flows near $x = 0$ should be close to the similarity ones with $U_w = x$, and besides, the flows as $x \to +\infty$ should be close to the similarity ones with $U_w = 1/2$,

respectively. For similarity flows with $U_w = x$ and 1/2, the similarity variables are $y/\sqrt{\nu}$ and $y/\sqrt{\nu x}$, respectively. Therefore, according to the definition (15) of the variable η, we choose

$$\sigma(x) = \sqrt{1+x},$$

which tends to $y/\sqrt{\nu}$ as $x \to 0$, and to $y/\sqrt{\nu x}$ as $x \to +\infty$, respectively. Similarly, we define

$$\xi = \Gamma(x) = \frac{x}{1+x},$$

which gives

$$U_w = \xi, \quad \sigma_1(\xi) = \frac{1}{2}, \quad \sigma_2(\xi) = 1 - \xi.$$

Note that $\sigma(x)$ and $\Gamma(x)$ are the same as those defined in Example 1.

Similarly, the corresponding series solutions $f_{\eta\eta}(\xi, 0)$ is a power function of $\hbar$ that influences the convergence of the solution series. In a similar way, by plotting the curve $f_{\eta\eta}(\xi, 0) \sim \hbar$ for different values of $\xi \in [0, 1]$, it is found that the series $f_{\eta\eta}(\xi, 0)$ converges in the whole region $\xi \in [0, 1]$ when $\hbar = -1/2$. Furthermore, it is found that, when $\hbar = -1/2$, the series of $f(\xi, \eta)$ is also convergent in the whole region $\xi \in [0, 1]$ and $0 \leqslant \eta < +\infty$. Our convergent series solution gives

$$C_f(x) \to -2\sqrt{\nu}/x, \quad \delta(x) \to \sqrt{\nu} \quad \text{as } x \to 0$$

and

$$C_f(x) \to -1.2551\sqrt{\nu/x}, \quad \delta(x) \to 2.28537\sqrt{\nu x} \quad \text{as } x \to +\infty.$$

Note that, for similarity flows, it holds

$$C_f(x) = -2\sqrt{\nu}/x, \quad \delta(x) = \sqrt{\nu}, \quad \text{when } U_w = x \tag{50}$$

and

$$C_f(x) = -1.2551\sqrt{\nu/x}, \quad \delta(x) = 2.28537\sqrt{\nu x}, \quad \text{when } U_w = 1/2. \tag{51}$$

Thus, the non-similarity flows in the region $x \to 0$ and $+\infty$ are very close to the similarity ones in case of $U_w = x$ and 1/2, respectively. However, the flows in the region $0.1 < x < 100$ are non-similar, as shown in Figs. 5 and 6.

The above two examples illustrate the validity of our analytic approach. Note that the two examples uses the same transformation $\xi = \Gamma(x) = x/(1+x)$. However, it should be emphasized that, if $\Gamma(x) = x$, then $\xi = x$ and $U_w(\xi) = U_w(x)$. So, our approach described in Section 2 is valid for any sheet stretching velocity $U_w(x)$ in general.

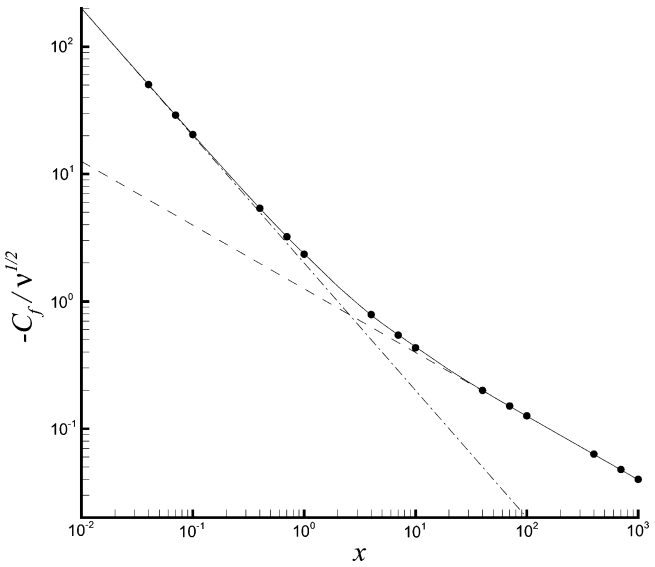

Fig. 5. The local coefficient of skin friction $C_f(x)/\sqrt{\nu}$ of non-similarity flows in case of $U_w = x/(1+x) - 0.5x^2/(1+x)^2$. Solid-line: 30th-order HAM result; symbols: 20th-order HAM result; dashed-line: $C_f(x) = -1.2551\sqrt{\nu/x}$; dash-dotted line: $C_f(x) = -2\sqrt{\nu}/x$.

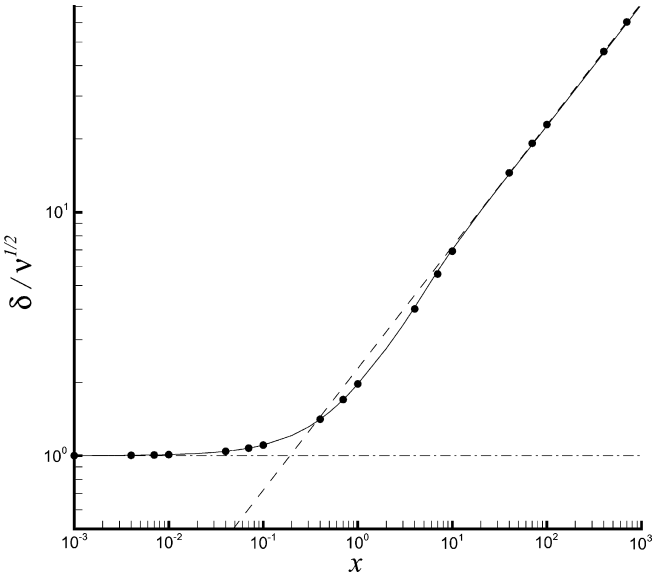

Fig. 6. The boundary-layer thickness $\delta(x)/\sqrt{\nu}$ of non-similarity flows in case of $U_w = x/(1+x) - 0.5x^2/(1+x)^2$. Solid-line: 30th-order HAM result; symbols: 20th-order HAM result; dashed-line: $\delta(x) = 2.28537\sqrt{\nu x}$; dash-dotted line: $\delta(x) = \sqrt{\nu}$.

4. An approximate formula of skin friction

For the similarity flows in case of $U_w = ax^\lambda$, we have from (11) that

$$C_f(x) = k_f \sqrt{\frac{\nu}{\int_0^x U_w(z)\mathrm{d}z}}, \tag{52}$$

where k_f is only dependent upon λ. For example, $k_f = -1.4142$ when $U_w = ax$, and $k_f = -0.8875$ when $U_w = a$, as listed in Table 2.

As mentioned above, the two non-similarity flows tend to the similarity ones in case of $U_w = x$ (as $x \to 0$) and $U_w =$ constant (as $x \to +\infty$), respectively. Considering the fact that the similarity flows are special cases of non-similarity ones, it is straightforward to assume that the above formula is still a good approximation for non-similarity flows if one regards k_f as a function of x, i.e.,

$$C_f(x) \approx k_f(x) \sqrt{\frac{\nu}{\int_0^x U_w(z)\mathrm{d}z}}, \tag{53}$$

where the coefficient $k_f(x)$ is dependent upon $U_w(x)$. For the two examples considered in this paper, we have

Table 2
The coefficients k_f for similarity flows in case of $U_w = ax^\lambda$

λ	k_f
0	−0.8875
1/10	−0.9983
1/5	−1.0845
1/4	−1.1208
1/3	−1.1737
1/2	−1.2580
3/4	−1.3491
1	−1.4142
3/2	−1.5013
2	−1.5571
5/2	−1.5958
3	−1.6244
4	−1.6636
5	−1.6893
10	−1.7464

$$k_f(x) \to -1.414 \quad \text{as } x \to 0$$

and

$$k_f(x) \to -0.8875 \quad \text{as } x \to +\infty,$$

respectively. The above results give a line function k_f of $\xi = x/(1+x)$, i.e.,

$$k_f(x) = -1.414 + \frac{0.5265x}{1+x}. \tag{54}$$

Thus, for the two examples considered in this paper, we have

$$C_f(x) \approx \left(-1.414 + \frac{0.5265x}{1+x}\right)\sqrt{\frac{\nu}{\int_0^x U_w(z)\mathrm{d}z}}, \tag{55}$$

where

$$\int_0^x U_w(z)dz = x - \ln(1+x) \quad \text{for Example 1}$$

and

$$\int_0^x U_w(z)dz = \frac{x^2}{2(1+x)} \quad \text{for Example 2.}$$

It is interesting that, for two considered examples, the formula (55) gives rather good approximations of $C_f(x)$ in the whole region $0 < x < +\infty$, as shown in Figs. 7 and 8.

The above approach can be generalized. Assume that, as $x \to 0$, a non-similarity flow over a stretching sheet tends to a similarity flow whose skin friction is given by

$$C_f(x) = k_f^L\sqrt{\frac{\nu}{\int_0^x U_w(z)\mathrm{d}z}}, \tag{56}$$

and as $x \to +\infty$, it tends to the similarity ones whose skin friction is given by

$$C_f(x) = k_f^R\sqrt{\frac{\nu}{\int_0^x U_w(z)\mathrm{d}z}}. \tag{57}$$

Then, the local coefficient of skin friction of the non-similarity flow on the whole sheet $0 < x < +\infty$ is approximately given by

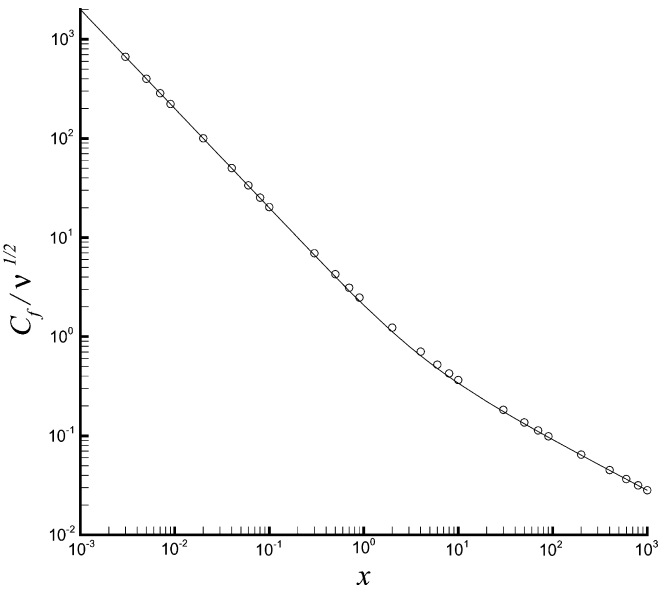

Fig. 7. Comparison of the approximate formula (55) with the exact result of $C_f(x)$ in case of $U_w = x/(1+x)$. Solid-line: 30th-order HAM result; symbols: formula (55).

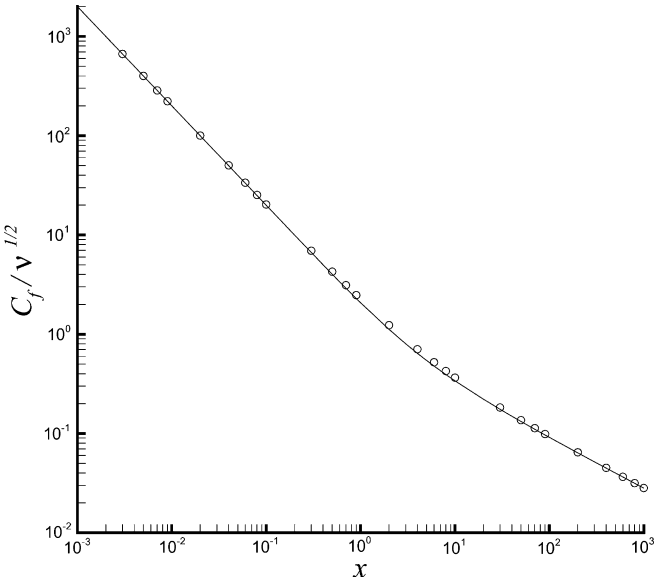

Fig. 8. Comparison of the approximate formula (55) with the exact result of $C_f(x)$ in case of $U_w = x/(1+x) - 0.5x^2/(1+x)^2$. Solid-line: 30th-order HAM result; symbols: formula (55).

$$C_f(x) \approx \left[k_f^L + (k_f^R - k_f^L)\frac{x}{1+x}\right]\sqrt{\frac{\nu}{\int_0^x U_w(z)\mathrm{d}z}}. \tag{58}$$

The coefficient k_f of similarity flows in case of $U_w = ax^\lambda$ is listed in Table 2. Using the formula (58) and Table 2, we can give good approximation of local coefficient of skin friction of non-similarity boundary-layer flows over a stretching sheet.

5. Discussions and conclusions

A analytic technique for strongly non-linear problems, namely the homotopy analysis method, is applied to propose a general approach to get convergent series solution of non-similarity boundary-layer flows. Without any assumptions of small/large quantities, the system of the *non-linear* partial differential equation with *variable* coefficients is transferred into an infinite number of *linear* ordinary differential equations with *constant* coefficients. Besides, an auxiliary artificial parameter is used to ensure the convergence of the series solution. To show the validity of this approach, two typical non-similarity flows are investigated. Different from previous analytic results, our series solutions are convergent and valid for all physical variables in the whole domain of flows. Furthermore, the relationship between the non-similarity and similarity boundary-layer flows is studied. It is found that, for the considered two non-similarity boundary-layer flows, the so-called local similarity exists only near $x = 0$ and as $x \to +\infty$. Using this kind of relationship, one approximate formula of the local coefficient of skin friction for non-similarity flows is given, which agrees with the convergent series solutions for all physical parameters and variables.

Note that the original non-linear PDE (19) contains derivatives with respect to both η and ξ. However, we choose an auxiliary linear operator (45) which only contains the derivatives with respect to η. Mathematically, this is mainly because the homotopy analysis method provides us great freedom to choose the auxiliary linear operator. More importantly, it also provides us a simple way to ensure the convergence of solution series by means of choosing a proper value of the convergence-control parameter $\hbar$: the freedom on the choice of the auxiliary linear operator has no meanings if one cannot ensure the convergence of solution series. It is interesting that Liao and Pop [43] used the *same* auxiliary linear operator to solve *similarity* boundary-layer flows. Thus, in the frame of the homotopy analysis method, the non-similarity boundary-layer flows can be solved in a similar way like similarity boundary-layer flows. Physically, it is mainly because the boundary-layer flow exists: the velocity variation across the flow direction is much larger than that in the flow direction. Thus, one can apply this analytic approach to solve different types of non-similarity boundary-layer flows in a similar way.

From mathematical point of view, this analytic approach is even more general in principle and can be applied to solve different types of non-linear PDEs (or ODEs) with variable coefficients in science and engineering.

Acknowledgements

This work is partly supported by National Natural Science Foundation of China (Approval Nos. 10572095 and 50739004), Program for Changjiang Scholars and Innovative Research Team in University (Approval No. IRT0525), and National 863 Plan Project of China (Approval No. 2006AA09Z354).

References

[1] Prandtl L. Über Flüssigkeitsbewegungen bei sehr kleiner Reibung. Verhandlg. In: III Int. Math. Kongr.; 1904. p. 484–491.
[2] Blasius H. Grenzschichten in Füssigkeiten mit kleiner Reibung. Z Math Phys 1908;56:1–37.
[3] Howarth L. On the solution of the laminar boundary layer equations. Proc R Soc Lond A 1938;164:547–79.
[4] Van Dyke M. Higher approximations in boundary-layer theory. Part 1: General analysis. J Fluid Mech 1962;14:161–77.
[5] Van Dyke M. Higher approximations in boundary-layer theory. Part 2: Applications to leading edges. J Fluid Mech 1962;14:481–95.
[6] Van Dyke M. Higher approximations in boundary-layer theory. Part 3: Parabola in uniform stream. J Fluid Mech 1964;19:145–59.
[7] Van Dyke M. Higher-order boundary-layer theory. Annu Rev Fluid Mech 1969;1:265–92.
[8] Van Dyke M. Perturbation methods in fluid mechanics. Stanford: The Parabolic Press; 1975.
[9] Tani I. History of boundary-layer theory. Annu Rev Fluid Mech 1977;9:87–111.
[10] Schlichting H, Gersten K. Boundary layer theory. Berlin: Springer; 2000.
[11] Sobey IJ. Introduction to interactive boundary layer theory. Oxford University Press; 2000.
[12] Crane L. Flow past a stretching plate. Z Angew Math Phys 1970;21:645–7.
[13] Banks WHH. Similarity solutions of the boundary-layer equations for a stretching wall. J Mech Theor Appl 1983;2:375–92.
[14] Banks WHH, Zaturska MB. Eigensolutions in boundary-layer flow adjectent to a stretching wall. IMA J Appl Math 1986;36:263–73.
[15] Grubka LJ, Bobba KM. Heat transfer characteristics of a continuous stretching surface with variable temperature. ASME J Heat Transfer 1985;107:248–50.
[16] Ali ME. Heat transfer characteristics of a continuous stretching surface. Wärme und Stoffübertragung 1994;29:227–34.
[17] Erickson LE, Fan LT, Fox VG. Heat and mass transfer on a moving continuous flat plate with suction or injection. Indust Eng Chem 1966;5: 19–25.
[18] Gupta PS, Gupta AS. Heat and mass transfer on a stretching sheet with suction or blowing. Can J Chem Eng 1977;55:744–6.
[19] Chen CK, Char MI. Heat and mass transfer on a continuous stretching surface with suction or blowing. J Math Anal Appl 1988;135:568–80.
[20] Chaudhary MA, Merkin JH, Pop I. Similarity solutions in the free convection boundary-layer flows adjacent to vertical permeable surfaces in porous media. Eur J Mech B: Fluids 1995;14:217–37.
[21] Elbashbeshy EMA. Heat transfer over a stretching surface with variable surface heat flux. J Phys D: Appl Phys 1998;31:1951–4.
[22] Magyari E, Keller B. Exact solutions for self-similar boundary-layer flows induced by permeable stretching walls. Eur J Mech B: Fluids 2000;19: 109–22.
[23] Görtler H. Eine neue Reihenentwicklung für laminare Grenzschichten. ZAMM 1952;32:270–1.
[24] Wanous KJ, Sparrow EM. Heat transfer for flow longitudinal to a cylinder with surface mass transfer. J Heat Transfer Trans Ser C 1965;87(1): 317–9.
[25] Catherall D, Stewartson, Williams. Viscous flow past a flat plate with uniform injection. Proc R Soc A 1965;284:370–96.
[26] Sparrow EM, Quack H. Local non-similarity boundary-layer solutions. AIAA J 1970;8(11):1936–42.
[27] Sparrow EM, Yu HS. Local non-similarity thermal boundary-layer solutions. J Heat Transfer Trans ASME 1971:328–34.
[28] Massoudi M. Local non-similarity solutions for the flow of a non-Newtonian fluid over a wedge. Int J Non-Linear Mech 2001;36:961–76.
[29] Cimpean D, Merkin JH, Ingham DB. On a free convection problem over a vertical flat surface in a porous medium. Transport Porous 2006;64: 393–411.
[30] Gorla RSR, Kumari M. Non-similar solutions for mixed convection in non-Newtonian fluids along a vertical plate in a porous medium. Transport Porous 1998;33:295–307.
[31] Duck PW, Stow SR, Dhanak MR. Non-similarity solutions to the corner boundary-layer equations (and the effects of wall transpiration). J Fluid Mech 1999;400:125–62.
[32] Sahu AK, Mathur MN, Chaturani P, Bharatiya SS. Momentum and heat transfer from a continuous moving surface to a power-law fluid. Acta Mech 2000;142:119–31.
[33] Banu N, Rees DAS. The effect of inertia on vertical free convection boundary-layer flows from a heated surface in porous medium with suction. Int Commun Heat Mass Transfer 2000;27(6):775–83.
[34] Char MI, Lin JD, Chen HT. Conjugate mixed convection laminar non-Darcy film condensation along a vertical plate in a porous medium. Int J Eng Sci 2001;39:897–912.
[35] Cheng WT, Lin HT. Non-similarity solution and correlation of transient heat transfer in laminar boundary layer flow over a wedge. Int J Eng Sci 2002;40(5):531–48.
[36] Chen CH. Combined heat and mass transfer in MHD free convection from a vertical surface with Ohmic heating and viscous disserpation. Int J Eng Sci 2004;42:699–713.
[37] Roy S, Datta P, Mahanti NC. Non-similar solution of an unsteady mixed convection flow over a vertical cone with suction or injection. Int J Heat Mass Transfer 2007;50:181–7.
[38] Liao SJ. Beyond perturbation: introduction to the homotopy analysis method. Boca Raton: Chapman & Hall/CRC Press; 2003.
[39] Liao SJ. On the analytic solution of magnetohydrodynamic flows of non-Newtonian fluids over a stretching sheet. J Fluid Mech 2003;488: 189–212.
[40] Liao SJ. Series solutions of unsteady boundary-layer flows over a stretching flat plate. Stud Appl Math 2006;117(3):2529–39.
[41] Liao SJ, Tan Y. A general approach to obtain series solutions of nonlinear differential equations. Stud Appl Math 2007;119:297–355.
[42] Liao SJ. Notes on the homotopy analysis method: Some definitions and theorems. Commun Nonlinear Sci Numer Simulat 2009;14:983–97.
[43] Liao SJ, Pop I. Explicit analytic solution for similarity boundary layer equations. Int J Heat Mass Transfer 2004;47(1):75–85.
[44] Yamashita M, Yabushita K, Tsuboi K. An analytic solution of projectile motion with the quadratic resistance law using the homotopy analysis method. J Phys A 2007;40:8403–16.
[45] Bouremel Y. Explicit series solution for the Glauert-jet problem by means of the homotopy analysis method. Commun Nonlinear Sci Numer Simul 2007;12(5):714–24.
[46] Abbasbandy S. The application of the homotopy analysis method to solve a generalized Hirota–Satsuma coupled KdV equation. Phys Lett A 2007;361:478–83.
[47] Abbasbandy S. Homotopy analysis method for heat radiation equations. Int Commun Heat Mass Transfer 2007;34:380–7.
[48] Hayat T, Sajid M. On analytic solution for thin film flow of a forth grade fluid down a vertical cylinder. Phys Lett A 2007;361:316–22.
[49] Hayat T, Sajid M. Analytic solution for axisymmetric flow and heat transfer of a second grade fluid past a stretching sheet. Int J Heat Mass Transfer 2007;50:75–84.
[50] Allan FM. Derivation of the Adomian decomposition method using the homotopy analysis method. Appl Math Comput 2007;190:6–14.
[51] Sajid M, Hayat T, Asghar S. On the analytic solution of the steady flow of a fourth grade fluid. Phys Lett A 2006;355:18–26.
[52] Zhu SP. A closed-form analytical solution for the valuation of convertible bonds with constant dividend yield. ANZIAM J 2006;47:477–94.
[53] Zhu SP. An exact and explicit solution for the valuation of American put options. Quant Finance 2006;6:229–42.
[54] Liao SJ. A new branch of solutions of boundary-layer flows over an impermeable stretched plate. Int J Heat Mass Transfer 2005;48(12): 2529–39.
[55] Liao SJ, Magyari E. Exponentially decaying boundary layers as limiting cases of families of algebraically decaying ones. ZAMP 2006;57(5): 777–92.
[56] Cheng J, Cang J, Liao SJ. On the interaction of deep water waves and exponential shear currents. ZAMP, in press.

[57] Adomian G. Nonlinear stochastic differential equations. J Math Anal Appl 1976;55:441–52.
[58] Adomian G. Solving frontier problems of physics: the decomposition method. Boston and London: Kluwer Academic Publishers; 1994.
[59] Wazwaz AM. The decomposition method applied to systems of partial differential equations and to the reaction–diffusion Brusselator model. Appl Math Comput 2000;110:251–64.
[60] Ramos JI, Soler E. Domain decomposition techniques for reaction–diffusion equations in two-dimensional regions with re-entrant corners. Appl Math Comput 2001;118:189–221.
[61] Karmishin AV, Zhukov AT, Kolosov VG. Methods of dynamics calculation and testing for thin-walled structures. Moscow: Mashinostroyenie; 1990 [in Russian].
[62] Awrejcewicz J, Andrianov IV, Manevitch LI. Asymptotic approaches in nonlinear dynamics. Berlin: Springer-Verlag; 1998.
[63] Lyapunov AM. General problem on stability of motion. Taylor & Francis, London, 1992 [English translation] [1892].